Dear Dr. Luterbacher,

My coauthors and I thank you for your invitation to revise our manuscript. Here we will comment on, one-by one, the referee comments/suggestions.

Sincerely,
Nesibe Köse

1. For Figure 9: we calculated the field significance and plot the significant areas on the maps. For Figure 8, almost all areas were significant. So, we added a short text to Figure capture about significant areas.
2. We added more text to the capture of Figure 4 (now 3) and 10.
3. We created anew figure for Figure 6.
4. We included a text to conclusion part concluding comparison with existing spatial reconstructions.
5. We changed the Abstract based on your suggestions.

Spring temperature variability over Turkey since 1800 CE reconstructed from a broad network of tree-ring data

Nesibe Köse[(1),*], H. Tuncay Güner[(1)], Grant L. Harley[(2)], Joel Guiot[(3)]

[(1)]Istanbul University, Faculty of Forestry, Forest Botany Department 34473 Bahçeköy-Istanbul, Turkey
[(2)]University of Southern Mississippi, Department of Geography and Geology, 118 College Drive Box 5051, Hattiesburg, Mississippi, 39406, USA
[(3)] Aix-Marseille Université, CNRS, IRD, CEREGE UM34, ECCOREV, 13545 Aix-en-Provence, France

*Corresponding author. Fax: +90 212 226 11 13
E-mail address: nesibe@istanbul.edu.tr

Abstract

~~The 20^{th} century was marked by significant decreases in spring temperature ranges and increased nighttime temperatures throughout Turkey.~~ The meteorological observational period in Turkey, which starts *ca.* ~~1929~~ 1930 CE, is too short for understanding long-term climatic variability. Tree rings ~~, as proxy records,~~ have been used intensively as proxy records to understand summer precipitation history of the region, primarily because of having a dominant precipitation signal. ~~But still~~Yet,~~Hence~~, the historical context of ~~this gradual warming trend in spring temperatures~~temperature variability is unclear. Here we used higher order principle components of a network of 23 tree-ring chronologies to provide a high-resolution spring (March–April) temperature reconstruction over Turkey during the period 1800–2002. The reconstruction model accounted for 67% (Adj. $R^2 = 0.64$, $p < 0.0001$) of the instrumental temperature variance over the full calibration period (1930–2002). ~~During the pre-instrumental period (1800–1929) we captured more cold events (*n* = 23) than warm (*n* = 13), and extreme cold and warm events were typically of short duration (1–2 years). Compared to coeval reconstructions of precipitation in the region, our results are similar with durations of extreme wet and dry events.~~ The reconstruction is punctuated by a temperature increase during the 20^{th} century; yet extreme cold and warm events during the 19^{th} century seem to eclipse conditions during the 20^{th} century. ~~During the 19^{th} century, annual temperature ranges are more volatile and characterized by more short-term fluctuations compared to the 20^{th} century~~. ~~During the period 1900–2002, our reconstruction shows a gradual warming trend, which includes the period during which diurnal temperature ranges decreased as a result of increased urbanization in Turkey.~~ ~~Comparisons with instrumental gridded data and spatial climate reconstructions offered independent validation of this study and revealed the potential for reconstructing temperature in an unlikely area, especially given the~~

~~strong precipitation signals displayed by most tree species growing in the dry Mediterranean climate.~~ We found significant correlations between our March–April spring temperature reconstruction and existing gridded spring temperature reconstructions for Europe over Turkey and southeastern Europe. Moreover, the precipitation signal obtained from the tree-ring network (first principle component) showed highly significant correlations with gridded summer drought index reconstruction over Turkey and Mediterranean countries. Our results showed that, beside the dominant precipitation signal, a temperature signal can be extracted from tree-ring series and ~~having temperature signal, beside dominant precipitation signal, can~~they can be useful proxies to reconstruct past temperature variability.

KEYWORDS: Dendroclimatology, Climate reconstruction, *Pinus nigra*, Principle component analysis, Spring temperature.

1 Introduction

An extensive body of literature details climate changes in the Mediterranean region over the last two millennia (*c.f.* Lionello, P. (Ed.), 2012). Paleolimnological studies provide evidence that the Medieval Climatic Anomaly (MCA; 900–1300 CE) characterized warm and dry conditions over the Iberian Peninsula, while the Little Ice Age (LIA; 1300–1850 CE) brought opposite climate conditions, forced by interactions between the East Atlantic and North Atlantic Oscillation (Sanchez-Lopez et al. 2016). In addition, Roberts et al. (2012) highlighted an intriguing spatial dipole NAO pattern between the western and eastern Mediterranean region, which brought anti-phased warm (cool) and wet (dry) conditions during the MCA and LIA. The hydro-climate patterns revealed by previous investigations appear to have been forced not only by NAO, but other climate modes with non-stationary teleconnections across the region (Roberts et al. 2012).

Significant decreases in spring diurnal temperature ranges (DTR) occurred throughout Turkey from 1929 to 1999 (Turkes & Sumer 2004). This decrease in spring DTRs was characterized by day-time temperatures that remained relatively constant while a significant increase in night-time temperatures were recorded over western Turkey and were concentrated around urbanized and rapidly-urbanizing cities. The historical context of this gradual warming trend in spring temperatures is unclear as the high-quality meteorological records in Turkey, which start in 1930s, are relatively short for understanding long-term climatic variability.

~~An extensive body of literature details climate changes in the Mediterranean region over the last two millennia (*c.f.* Lionello, P. (Ed.), 2012). Paleolimnological studies provide evidence that the~~

~~Medieval Climatic Anomaly (MCA; 900–1300 CE) characterized warm and dry conditions over the Iberian Peninsula, while the Little Ice Age (LIA; 1300–1850 CE) brought opposite climate conditions, forced by interactions between the East Atlantic and North Atlantic Oscillation (Sanchez-Lopez et al. 2016). In addition, Roberts et al. (2012) highlighted an intriguing spatial dipole NAO pattern between the western and eastern Mediterranean region, which brought anti-phased warm (cool) and wet (dry) conditions during the MCA and LIA. The hydro-climate patterns revealed by previous investigations appear to have been forced not only by NAO, but other climate modes with non-stationary teleconnections across the region (Roberts et al. 2012).~~

Tree rings have shown to provide useful information about the past climate of Turkey and were used intensively during the last decade to reconstruct precipitation in the Aegean (Griggs et al. 2007), Black Sea (Akkemik et al. 2005, 2008; Martin-Benitto et al. 2016), Mediterranean regions (Touchan et al. 2005a), as well as the Sivas (D'Arrigo & Cullen 2001), southwestern (Touchan et al. 2003, Touchan et al. 2007; Köse et al. 2013), south-central (Akkemik & Aras 2005) and western Anatolian (Köse et al. 2011) regions of Turkey. These studies used tree rings to reconstruct precipitation because available moisture is often found to be the most important limiting factor that influences radial growth of many tree species in Turkey. These studies revealed past spring-summer precipitation, and described past dry and wet events and their duration. Recently, Cook et al. (2015) presented Old World Drought Atlas (OWDA), which is a set of year by year maps of reconstructed Palmer Drought Severity Index from tree-ring chronologies over the Europe and Mediterranean Basin. Heinrich et al. (2013) provided a winter-to-spring temperature proxy for Turkey from carbon isotopes within the growth rings of *Juniperus excelsa* M. Bieb. since AD 1125. Low-frequency temperature trends corresponding to the end of Medieval Climatic Anomaly and Little Ice Age were identified in the record, but the proxy failed to identify the recent warming trend during the 20th century. In this study, we present a tree-ring based spring temperature reconstruction from Turkey and compare our results to previous reconstructions of temperature and precipitation to provide a more comprehensive understanding of climate conditions during the 19th and 20th centuries.

2 Data and Methods

2.1 Climate of the Study Area

The study area, which spans 36–42º N and 26–38º E, was based on the distribution of available tree-ring chronologies. This vast area covers much of western Anatolia and includes the western Black Sea, Marmara, and western Mediterranean regions. Much of this area is characterized by a Mediterranean climate that is primarily controlled by polar and tropical air masses (Türkeş 1996a, Deniz et al. 2011). In winter, polar fronts from the Balkan Peninsula bring cold air that is centered in the Mediterranean. Conversely, the dry, warm conditions in summer are dominated by weak frontal systems and maritime effects. Moreover, the Azores high-pressure system in summer and anticyclonic activity from the Siberian high-pressure system often cause below normal precipitation and dry sub-humid conditions over the region (Türkeş 1999, Deniz et al. 2011). In this Mediterranean climate, annual mean temperature and precipitation range from 3.6 °C to 20.1 °C and from 295 to 2220 mm, respectively, both of which are strongly controlled by elevation (Deniz et al. 2011).

2.2 Development of tree-ring chronologies

To investigate past temperature conditions, we used a network of 23 tree-ring site chronologies (Fig. 1). Fifteen chronologies were produced by previous investigations (Mutlu et al. 2011, Akkemik et al. 2008, Köse et al. unpublished data, Köse et al. 2011, Köse et al. 2005) that focused on reconstructing precipitation in the study area. In addition, we sampled eight new study sites and developed tree-ring time series for these areas (Table 1). Increment cores were taken from living *Pinus nigra* Arnold and *Pinus sylvestris* L. trees and cross-sections were taken from *Abies nordmanniana* (Steven) Spach and *Picea orientalis* (L.) Link trunks.

Samples were processed using standard dendrochronological techniques (Stokes & Smiley 1968, Orvis & Grissino-Mayer 2002, Speer 2010). Tree-ring widths were measured, then visually crossdated using the list method (Yamaguchi 1991). We used the computer program COFECHA, which uses segmented time-series correlation techniques, to statistically confirm our visual crossdating (Holmes 1983, Grissino-Mayer 2001). Crossdated tree-ring time series were then standardized by fitting a 67% cubic smoothing spline with a 50% cutoff frequency to remove non-climatic trends related to the age, size, and the effects of stand dynamics using the ARSTAN program (Cook 1985, Cook et al. 1990a). These detrended series were then pre-whitened with low-order autoregressive models to produce time series with a strong common signal and without biological persistence. These series may be more suitable to understand the effect of climate on tree-growth, even if any persistence due to climate might be removed by pre-whitening. For each chronology, the individual series were averaged to a single chronology by computing the biweight robust means to reduce the influences of outliers (Cook et al. 1990b). In this research we used residual chronologies obtained from ARSTAN to reconstruct temperature.

The mean sensitivity, which is a metric representing the year-to-year variation in ring width (Fritts 1976), was calculated for each chronology and compared. The minimum sample depth for each chronology was determined according to expressed population signal (EPS), which we used as a guide for assessing the likely loss of reconstruction accuracy. Although arbitrary, we required the commonly considered threshold of EPS > 0.85 (Wigley et al. 1984; Briffa & Jones 1990).

2.3 Identifying relationship between tree-ring width and climate

We extracted high resolution monthly temperature and precipitation records from the climate dataset CRU TS 3.23 gridded at 0.5º intervals (Jones and Harris 2008) from KNMI Climate Explorer (http://climexp.knmi.nl) for 36–42 ºN, 26–38 ºE. The period AD 1930–2002 was chosen for the analysis because it maximized the number of station records within the study area.

First, the climate-growth relationships were investigated with response function analysis (RFA) (Fritts 1976) for biological year from previous October to current October using the DENDROCLIM2002 program (Biondi & Waikul 2004). This analysis is done to determine the months during which the tree-growth is the most responsive to temperature. RFA results showed that precipitation from May to August and temperature in March and April have dominant control on tree-ring formation in the area. Second, we produced correlation maps showing correlation coefficients between tree-ring chronologies and the climate factors most important for tree growth, which are May–August precipitation and March–April temperature, to find the spatial structure of radial growth-climate relationship (St. George 2014, St. George and Ault 2014, Hellmann et al. 2016). For each site we used the closest gridded temperature and precipitation values.

2.4 Temperature reconstruction

The climate reconstruction is performed by regression based on the principal component (PCs) of the 23 chronologies within the study area. Principle Component Analysis (PCA) was done over the entire period in common to the tree-ring chronologies. The significant PCs were selected by stepwise regression. We combined forward selection with backward elimination setting *p* < ~~≤~~0.05 as entrance tolerance and *p* < ~~≤~~0.10 as exit tolerance. The final model obtained when the regression reaches a local minimum of the root mean squared error (RMSE). The order of entry of the PCs into the model was PC_3, PC_{21}, PC_4, PC_{15}, PC_5, PC_{17}, PC_7, PC_9, PC_{10}. The regression equation is calibrated on the common period (1930–2002) between robust temperature time-series and the selected tree-ring series. Third, the final reconstruction is based on bootstrap regression (Till and Guiot~~,~~ 1990), a method designed to calculate appropriate confidence intervals for reconstructed values and explained variance even in cases of short time-series. It consists in randomly resampling the calibration datasets to produce 1000 calibration equations based on a number of slightly different datasets.

The quality of the reconstruction is assessed by a number of standard statistics. The overall quality of fit of reconstruction is evaluated based on the determination coefficient (R^2), which expresses the percentage of variance explained by the model and ~~the root mean squared error~~

Biçimlendirilmiş: Yazı tipi: İtalik

Biçimlendirilmiş: Yazı tipi: İtalik

Biçimlendirilmiş: Yazı tipi: İtalik

~~(~~RMSE~~)~~, which expresses the calibration error. This does not insure the quality of the extrapolation which needs additional statistics based on independent observations, i.e. observations not used by the calibration (verification data). They are provided by the observations not resampled by the bootstrap process. The prediction RMSE (called RMSEP), the reduction of error (RE) and the coefficient of efficiency (CE) are calculated on the verification data and enable to test the predictive quality of the calibrated equations (Cook et al.~~,~~ 1994). Traditionally, a positive RE or CE values means a statistically significant reconstruction model, but bootstrap has the advantage to produce confidence intervals for such statistics without theoretical probability distribution and finally we accept the RE and CE for which the lower confidence margin at 95% are positive. This is more constraining than just accepting all positive RE and CE. For additional verification, we also present traditional split-sample procedure results that divided the full period into two subsets of equal length (Meko and Graybill~~,~~ 1995).

To identify the extreme March–April cold and warm events in the reconstruction, standard deviation (SD) values were used. Years one and two SD above and below the mean were identified as warm, very warm, cold, and very cold years, respectively., As a way to assess the spatial representation of our temperature reconstruction, we conducted a spatial field correlation analysis between reconstructed values and the gridded CRU TS3.23 temperature field (Jones and Harris 2008) for a broad region of the Mediterranean over the entire instrumental period (ca. 1930–2002). Finally, we compared our temperature reconstruction and also precipitation signal (PC1) against existing gridded temperature and hydroclimate reconstructions for Europe over the period 1800–2002. We performed spatial correlation analysis between [1] our temperature reconstruction and gridded temperature reconstructions for Europe (Xoplaki et al. 2005, Luterbacher et al. 2016) and OWDA (Cook et al. 2015); and [2] ~~2)~~ PC1 and summer precipitation reconstruction (Pauling et al., 2006) and Old World Drought Atlas (OWDA) (Cook et al. 2015).

2 Results and Discussion

2.1 Tree-ring chronologies

In addition to 15 chronologies developed by previous studies, we produced six *P. nigra*, one *P. sylvestris*, one *A. nordmanniana / P. orientalis* chronologies for this study (Table 2). The Çorum district produced two *P. nigra* chronologies: one the longest (KAR; 627 years long) and the other the most sensitive to climate (SAH; mean sensitivity value of 0.25). Previous investigations of climate-tree growth relationships reported a mean sensitivity range of 0.13–0.25 for *P. nigra* in Turkey (Köse 2011, Akkemik et al. 2008). The KAR, SAH, and ERC chronologies (with mean sensitivity values from 0.22 to 0.25) were classified as very sensitive, and the SAV, HCR, and PAY chronologies (mean sensitivity values range 0.17–0.18) contained values characteristic of being sensitive to climate. The lowest mean sensitivity value was obtained for the ART *A. nordmanniana / P. orientalis* chronology. Nonetheless, this chronology retained a statistically significant temperature signal ($p < 0.05$).

2.2 Tree-ring growth-climate relationship

RFA coefficients of May to August precipitation are positively correlated with most of the tree-ring series (Fig. 2) and among them, May and June coefficients are generally significant. The first principal component of the 23 chronologies, which explains 47% of the tree-growth variance, is highly correlated with May–August total precipitation, statistically ($r = 0.65$, p ~~≤~~ ≤

0.001) and visually (Fig. 3). The high correlation was expected given that numerous studies also found similar results in Turkey (Akkemik 2000a, Akkemik 2000b, Akkemik 2003, Akkemik et al. 2005, Akkemik et al. 2008, Akkemik & Aras 2005, Hughes et al. 2001, D'Arrigo & Cullen 2001, Touchan et al. 2003; Touchan et al. 2005a, Touchan et al. 2005b, Touchan et al. 2007, Köse et al. 2011, Köse et al. 2012, Köse et al. 2013, Martin-Benitto et al. 2016). The influence of temperature was not as strong as May–August precipitation on radial growth, although generally positive in early spring (March and April) (Fig. 2). Conversely, the ART chronology from northeastern Turkey contained a strong temperature signal, which was significantly positive in March.

Correlation maps representing influence of May-August precipitation (Fig. 4a) and March-April temperature (Fig 4b) also showed that strength of the summer precipitation signal is higher and significant almost all over the Turkey. Higher precipitation in summer has a positive effect on tree-growth, because of long-lasting dry and warm conditions over the Turkey (Türkeş 1996b, Köse et al. 2012). Spring precipitation signal are generally positive and significant only for four tree-ring sites. The sites located at the upper distributions of the species are generally showed higher correlations. The highest correlations obtained for *Picea/Abies* chronology (ART) from the Caucasus, and for *Pinus nigra* chronology (HCR) from the upper (about 1900 m) and southeastern distribution of the species. This black pine forest was still partly covered by snow from previous year during the field work in fall. Higher temperatures in spring maybe cause snow melt earlier and lead to produce larger annual rings. In addition to these chronologies, we also used the chronologies that revealed the influence of precipitation, as well as temperature to reconstruct March–April temperature.

2.3 March-April temperature reconstruction

The higher order PCs of the 23 chronologies are significantly correlated with the March–April temperature and, by nature, are independent on the precipitation signal (Table 3). The best selection for fit temperature are obtained with the PC_3, PC_4, PC_5, PC_7, PC_9, PC_{10}, PC_{15}, PC_{17}, PC_{21}, which explains together 25% of the tree-ring chronologies. So the temperature signal remains important in the tree-ring chronologies and can be reconstructed. The advantage to separate both signals through orthogonal PCs enable to remove an unwanted noise for our temperature reconstruction. Thus, PC_1 was not used as potential predictor of temperature because it is largely dominated by precipitation (Table 3, Fig. 3). The last two PCs contain a too small part of the total variance to be used in the regressions. However, even if Jolliffe (1982) and Hadi & Ling (1998) claimed that certain PCs with small eigenvalues (even the last one), which are commonly ignored by principal components regression methodology, may be related to the independent variable, we must be cautious with that because they may be much more dominated by noise than the first ones. So, the contribution of each PC to the regression sum of squares is also important for selection of PCs (Hadi & Ling 1998). The findings of Jolliffe (1982) and Hadi & Ling (1998) provide a justification for using non-primary PCs, (*e.g.*, of second and higher order) in our regression, given that correlations with temperature may be over-powered by affects from precipitation in our study area (Cook 2011, personal communication).

Using this method, the calibration and verification statistics indicated a statistically significant reconstruction (Table 4, Fig. 5). For additional verification, we also present split-sample procedure results. Similarly bootstrap results, the derived calibration and verification tests using this method indicated a statistically significant RE and CE values (Table 5).

The regression model accounted for 67% (Adj. $R^2 = 0.64$, $p \cancel{\leq} < 0.0001$) of the actual temperature variance over the calibration period (1930–2002). Also, actual and reconstructed March–April temperature values had nearly identical trends during the period 1930–2002 (Fig. 5). Moreover, the tree-ring chronologies successfully simulated both high frequency and warming trends in the temperature data during this period. The reconstruction was more powerful at classifying warm events rather than cold events. Over the last 73 years, eight of ten warm events in the instrumental data were also observed in the reconstruction, while five of nine cold events were captured. Similarly, previous tree-ring based precipitation reconstructions for Turkey (Köse et al. 2011; Akkemik et al. 2008) were generally more successful in capturing dry years rather than wet years.

Biçimlendirilmiş: Yazı tipi: İtalik

Biçimlendirilmiş: Yazı tipi: İtalik

Our temperature reconstruction on the 1800–2002 period is obtained by bootstrap regression, using 1000 iterations (Fig. 6). The confidence intervals are obtained from the range between the 2.5^{th} and the 97.5^{th} percentiles of the 1000 simulations. For the pre-instrumental period (1800–1929), a total of 23 cold (1813, 1818, 1821, 1824, 1837, 1848, 1854, 1858, 1860, 1869, 1877–1878, 1880–1881, 1883, 1897–1898, 1905–1907, 1911–1912, 1923) and 13 warm (1801–1802, 1807, 1845, 1853, 1866, 1872–1873, 1879, 1885, 1890, 1901, 1926) events were determined. After comparing our results with event years obtained from May–June precipitation reconstructions from western Anatolia (Köse et al. 2011), the cold years 1818, 1848, and 1897 appeared to coincide with wet years and 1881 was a very wet year for the entire region.

Furthermore, these years can be described as cold (in March–April) and wet (in May–June) for western Anatolia.

Among the warm periods in our reconstruction, conditions during the year 1879 were dry, 1895 wet, and 1901 very wet across the broad region of western Anatolia (Köse et al. 2011). Hence, we defined 1879 as a warm (in March–April) and dry year (in May–June), and 1895 and 1901 were warm and wet years. In the years 1895 and 1901 the combination of a warm early spring and a wet late spring-summer caused enhanced radial growth in Turkey, interpreted as longer growing seasons without drought stress.

Of these event years, 1897 and 1898 were exceptionally cold and 1845, 1872 and 1873 were exceptionally warm. During the last 200 years, our reconstruction suggests that the coldest year was 1898 and the warmest year was 1873. The reconstructed extreme events also coincided with accounts from historical records. Server (2008) recounted the winter of 1898 as characterized by anomalously cold temperatures that persisted late into the spring season. A family, who brought their livestock herds up into the plateau region in Kırşehir seeking food and water were suddenly covered in snow on 11 March 1898. This account of a late spring freeze supports the reconstruction record of spring temperatures across Turkey, and offers corroboration to the quality of the reconstructed values.

Seyf (1985) reported that extreme summer temperature during the year 1873 resulted in widespread crop failure and famine. Historical documents recorded an infamous drought-derived famine that occurred in Anatolia from 1873 to 1874 (Quataert, 1996, Kuniholm, 1990), which claimed the lives of 250,000 people and a large number of cattle and sheep (Faroqhi, 2009). This drought caused widespread mortality of livestock and depopulation of rural areas through human mortality, and migration of people from rural to urban areas. Further, the German traveler Naumann (1893) reported a very dry and hot summer in Turkey during the year 1873 (Heinrich et al, 2013). Conditions worsened when the international stock exchanges crashed in 1873 (Zürcher, 2004). Our temperature record suggests that dry conditions during the early 1870s were possibly exacerbated by warm spring temperatures that likely carried into summer. A similar pattern of intensified drought by warm temperatures was demonstrated recently by Griffin and Anchukaitis (2014) for the current drought in California, USA.

Extreme cold and warm events were usually one year long, and the longest extreme cold and warm events were two and three years, respectively. These results were similar with durations of extreme wet and dry events in Turkey (Touchan et al. 2003, Touchan et al. 2005a, Touchan et al. 2005b, Touchan et al. 2007, Akkemik & Aras, 2005, Akkemik et al. 2005, Akkemik et al. 2008, Köse et al. 2011, Güner et al. 2016). Moreover, seemingly innocuous short-term warm events, such as the 1807 event, were recorded across the Mediterranean and in high elevations of the European regions. Casty et al. (2005) reported the year 1807 as being one of the warmest alpine summers in the European Alps over the last 500 years. As such, a drought record from Nicault et al. (2008) echoes this finding, as a broad region of the Mediterranean basin experienced drought conditions.

Low frequency variability of our spring temperature reconstruction showed larger variability in nineteenth century than twentieth century. Similar results observed on previous tree-ring based precipitation reconstructions from Turkey (Touchan et al. 2003, D’Arrigo et al. 2001, Akkemik and Aras 2005, Akkemik et al. 2005, Köse et al. 2011). Moreover, cold (warm) periods observed in our reconstruction are generally appeared as generally wet in the precipitation reconstructions, while rarely correlated with dry (wet) periods (Fig. 7). When we compare the relationship between temperature and precipitation over the instrumental period, both case, cold (warm) and wet (dry) as well as cold (warm) and dry (wet), can be observed.

Heinrich et al. (2013) analyzed winter-to-spring (January–May) air temperature variability in Turkey since AD 1125 as revealed from a robust tree-ring carbon isotope record from *Juniperus excelsa*. Although they offered a long-term perspective of temperature over Turkey, the reconstruction model, which covered the period 1949–2006, explained 27% of the variance in temperature since the year 1949. In this study, we provided a short-term perspective of temperature fluctuation based on a robust model (calibrated and verified 1930–2002; Adj. R^2 = 0.64; p ≤≤ 0.0001). Yet, the Heinrich et al. (2013) temperature record did not capture the 20th century warming trend as found elsewhere (Wahl et al. 2010). However, their temperature trend does agree with trend analyses conducted on meteorological data from Turkey and other areas in the eastern Mediterranean region. The warming trend seen during our reconstruction calibration period (1930–2002) was similar to the data shown by Wahl et al. (2010) across the region and hemisphere. Further, the warming trends seen in our record agrees with data presented by Turkes & Sumer (2004), of which they attributed to increased urbanization in Turkey. Considering long-term changes in spring temperatures, the 19th century was characterized by more high-frequency fluctuations compared to the 20th century, which was defined by more gradual changes and includes the beginning of decreased DTRs in the region (Turkes & Sumer 2004).

Biçimlendirilmiş: Yazı tipi: İtalik

Biçimlendirilmiş: Yazı tipi: İtalik

4 Comparison with instrumental gridded data and spatial reconstructions

Spatial correlation analysis revealed that our network-based temperature reconstruction was representative of conditions across Turkey, as well as the broader Mediterranean region (Fig. 8). During the period 1930–2002, estimated temperature values were highly significant (r range 0.5–0.6, $p < 0.01$) with instrumental conditions recorded from southern Ukraine to the west across Romania, and from northern areas of Libya and Egypt to the east across Iraq. The strength of the reconstruction model is evident in the broad spatial implications demonstrated by the temperature record. Thus, we interpret warm and cold periods and extreme events within the record with high confidence.

We compared our tree-ring based temperature reconstruction with existing gridded temperature reconstructions for Europe (Xoplaki et al. 2005, Luterbacher et al. 2016) and the Old World Drought Atlas (OWDA) (Cook et al. 2015) for further validation of the reconstruction (Fig.~~ure~~ 9a, b, c, respectively). Spatial correlations over the past 200 years were lower with reconstructed European summer temperature (May to July) (Fig. 9b). Yet, we expected this result because of the paucity of Turkey-derived proxies in the other reconstructions, as well as the differing seasons involved across the reconstructions. Similarly, our reconstruction showed weak correlations with summer drought index over Turkey. Beside comparing different seasons, perhaps this is because less precipitation begets drought conditions rather than high temperature in the region. The highest and significant (p < 0.05~~1~~) correlations were found with European spring (March to May) temperature reconstruction over ~~Turkey~~ southeastern Europe, which are stronger over Turkey (Fig. 9a). We used the mean of corresponding grid points from European spring temperature reconstruction over the study area (36–42º N, 26–38º E) to show how the correlation changed over time (Fig.~~ure~~ 10). The correlation coefficient was highly significant ($r = 0.76$, $p < 0.001$) during our calibration period (1930–2002). We found lower but still significant correlation ($r = 0.35$, $p < 0.10$) for the period of 1901–1929, which climatic records are very few over the region while available data has sufficient quality for most part of Europe. These results give additional verification for our reconstruction. Moreover, our reconstruction has a weak, insignificant relationship ($r = 0.13$, $p > 0.10$) during the 19th century. This may be related to poor reconstructive skill of European spring temperature reconstruction over Turkey, which contains few proxies from the country (Xoplaki et al. 2005, Luterbacher et al. 2004). Nonetheless, these results demonstrate that tree-ring chronologies from Turkey can serve as useful temperature proxies for further spatial temperature reconstructions to fill the gaps in the area.

We also compared the precipitation signal (PC1) obtained from our tree-ring network with Old World Drought Atlas (OWDA) (Cook et al. 2015) and gridded European summer precipitation reconstruction (Pauling et al., 2006) to test the strength of the signal spatially (Fig. 9d and e, respectively). We calculated highly significant positive correlations with summer drought index over Turkey and neighboring European countries such as Greece, Bulgaria, and Romania, while significant correlations are lover for the other Mediterranean countries (Fig. 9d). We found ~~positive but not so strong~~lover but still significant correlations over Turkey and Mediterranean countries with European summer precipitation reconstruction (Fig. 9e). Pauling et al. (2006) stated that poor reconstructive skills determined over Turkey because of few instrumental record before the1930s. These results showed that summer precipitation signal represented by PC1 is very strong not only on instrumental period, but also on pre-instrumental period, and represents a large spatial coverage.

4 Conclusions

In this study, we used a broad network of tree-ring chronologies to provide the first tree-ring based temperature reconstruction for Turkey and identified extreme cold and warm events during the period 1800–1929 CE. Similar to the precipitation reconstructions against which we compare our air temperature record, extreme cold and warm years were generally short in duration (one year) and rarely exceeded two-three years in duration. The coldest and warmest years over western Anatolia were experienced during the 19th century, and the 20th century is marked by a temperature increase.

Reconstructed temperatures for the 19th century suggest that more short-term fluctuations occurred compared to the 20th century. The gradual warming trend shown by our reconstruction calibration period (1930–2002) is coeval with decreases in spring DTRs. Given the results of Turkes and Sumer (2004), the variations in short- and long-term temperature changes between the 19th and 20th centuries might be related to increased urbanization in Turkey.

We highlight that the 20th century warming trend is unprecedented within the context of the past *ca.* 200 years, especially over the past *ca.* 15 years. Correlations with gridded climate fields and other climate reconstructions from the region revealed that our network-based temperature reconstruction was representative of conditions across Turkey, as well as the broader Mediterranean region. Expanding the tree-ring network across Turkey, especially to the east, will improve the spatial implications of future temperature reconstructions.

The study revealed the potential for reconstructing temperature in an area previously thought impossible, especially given the strong precipitation signals displayed by most tree species growing in the dry Mediterranean climate that characterizes broad areas of Turkey. Our reconstruction only spans 205 years due to the shortness of the common interval for the chronologies used in this study, but the possibility exists to extend our temperature reconstruction further back in time by increasing the sample depth with more temperature-sensitive trees, especially from northeastern Turkey. Thus future research will focus on increasing the number of tree-ring sites across Turkey, and maximizing chronology length at existing sites that would ultimately extend the reconstruction back in time.

Acknowledgements

This research was supported by The Scientific and Technical Research Council of Turkey (TUBITAK); Projects ÇAYDAG 107Y267 and YDABAG 102Y063. N. Köse was supported by The Council of Higher Education of Turkey. We are grateful to the Turkish Forest Service personnel and Ali Kaya, Umut Ç. Kahraman and Hüseyin Yurtseven for their invaluable support during our field studies. We thank to Dr. Ufuk Turuncoğlu for his help on spatial analysis. J. Guiot was supported by the Labex OT-Med (ANR-11-LABEX-0061), French National Research Agency (ANR).

References

Akkemik, Ü.: Dendroclimatology of Umbrella pine (*Pinus pinea* L.) in Istanbul (Turkey), Tree-Ring Bull., 56, 17–20, 2000a.

Akkemik, Ü.: Tree-ring chronology of *Abies cilicica* Carr. in the Western Mediterranean Region of Turkey and its response to climate, Dendrochronologia, 18, 73–81, 2000b.

Akkemik, Ü.: Tree-rings of *Cedrus libani* A. Rich the northern boundary of its natural distribution, IAWA J, 24(1), 63-73, 2003.

Akkemik ,Ü and Aras, A.: Reconstruction (1689–1994) of April–August precipitation in southwestern part of central Turkey, Int. J. Clim., 25, 537–548, 2005.

Akkemik, Ü., Dagdeviren, N., and Aras, A.: A preliminary reconstruction (A.D. 1635–2000) of spring precipitation using oak tree rings in the western Black Sea region of Turkey, Int. J. Biomet., 49(5), 297–302, 2005.

Akkemik, Ü., D'Arrigo, R., Cherubini, P., Köse, N., and Jacoby, G.: Tree-ring reconstructions of precipitation and streamflow for north-western Turkey, Int. J. Clim., 28, 173–183, 2008.

Biondi, F. and Waikul, K.: DENDROCLIM2002: A C++ program for statistical calibration of climate signals in tree-ring chronologies, Comp. Geosci., 30, 303–311, 2004.

Briffa, K. R. and Jones, P. D.: Basic chronology statistics and assessment. In: Methods of Dendrochronology: Applications in the Environmental Sciences (Cook, E. and Kairiukstis, L. A. eds). Kluwer Academic Publishers, Amsterdam, pp. 137–152, 1990.

Casty, C., Wanner, H., Luterbacher, J., Esper, J., and Böhm, R.: Temperature and precipitation variability in the European Alps since 1500, Int. J. Clim., 25(14), 1855–1880, 2005.

Cook, E.: A time series analysis approach to tree-ring standardization. PhD. Dissertation. University of Arizona, Tucson, 1985.

Cook, E., Briffa, K., Shiyatov, S., and Mazepa, V.: Tree-ring standardization and growth-trend estimation. In: Methods of Dendrochronology: Applications in the Environmental Sciences (Cook, E. and Kairiukstis, L. A. eds). Kluwer Academic Publishers, Amsterdam, pp.104–122, 1990a.

Cook, E., Shiyatov, S., and Mazepa, V.: Estimation of the mean chronology. In: Methods of Dendrochronology: Applications in the Environmental Sciences (Cook, E. and Kairiukstis, L. A. eds). Kluwer Academic Publishers, Amsterdam, pp. 123–132, 1990b.

Cook, E.R, Seager R., et al.: Old World megadroughts and pluvials during the Common Era. Sci. Adv., 1, e1500561, doi:10.1126/sciadv.1500561, 2015.

D’Arrigo, R. and Cullen, H. M.: A 350-year (AD 1628–1980) reconstruction of Turkish precipitation. Dendrochronologia ,19(2), 169–177, 2001.

Deniz, A., Toros, T., and Incecik, S.: Spatial variations of climate indices in Turkey, Int. J. Clim., 31, 394-403, 2011.

Fritts, H. C.: Tree Rings and Climate. Academic Press, New York, 1976.

Griggs, C., DeGaetano, A., Kuniholm, P., and Newton, M.: A regional high-frequency reconstruction of May–June precipitation in the north Aegean from oak tree rings, A.D. 1809–1989, Int. J. Clim., 27, 1075–1089, 2007.

Grissino-Mayer, H. D.: Evaluating crossdating accuracy: A manual and tutorial for the computer program COFECHA, Tree-Ring Res., 57, 205–221, 2001.

Griffin, D. and Anchukaitis, K. J.: How unusual is the 2012–2014 California drought? Geophy. Res. Lett., 41(24), 9017–9023, 2014.

Güner, H.T., Köse, N., Harley, G. L.: 200-year reconstruction of Kocasu River (Sakarya River Basin, Turkey) streamflow derived from a tree-ring network, Int. J. Biometeprol., DOI 10.1007/s00484-016-1223-y, 2016.

Hadi, A. S. and Ling, R. F.: Some cautionary notes on the use of principal components regression, Amer. Statist., 52(1), 15–19, 1998.

Heinrich, I., Touchan, R., Liñán, I. D., Vos, H., and Helle, G.: Winter-to-spring temperature dynamics in Turkey derived from tree rings since AD 1125, Clim. Dynam., 41(7–8), 1685–1701, 2013.

Hellmann, L., Agafonov, L., et al.: Diverse growth trends and climate responses across Eurasia's boreal forest. Environmental Research Letters: 11: 074021, doi:10.1088/1748-9326/11/7/074021.

Holmes, R. L.: Computer-assisted quality control in tree-ring data and measurements, Tree-Ring Bull., 43, 69–78, 1983.

Hughes, M. K., Kuniholm, P. I, Garfin, G. M., Latini, C., and Eischeid, J.: Aegean tree-ring signature years explained, Tree-Ring Res., 57(1), 67–73, 2001.

Jolliffe, I. T.: A note on the use of principal components in regression, Appl. Stat., 31(3), 300–303, 1982.

Jones, P. D. and Harris, I.: Climatic Research Unit (CRU) time-series datasets of variations in climate with variations in other phenomena. NCAS British Atmospheric Data Centre, 2008. http://catalogue.ceda.ac.uk/uuid/3f8944800cc48e1cbc29a5ee12d8542d

Köse, N., Akkemik, Ü., and Dalfes, H. N.: Anadolu'nun iklim tarihinin son 500 yılı: Dendroklimatolojik ilk sonuçlar. Türkiye Kuvaterner Sempozyumu-TURQUA–V, 02–03 Haziran 2005, Bildiriler Kitabı, 136–142 (In Turkish), 2005.

Köse, N., Akkemik, Ü., Dalfes, H. N., and Özeren, M. S.: Tree-ring reconstructions of May–June precipitation of western Anatolia, Quat. Res., 75, 438–450, 2011.

Köse, N., Akkemik, Ü., Dalfes, H. N., and Özeren, M. S., Tolunay D.: Tree-ring growth of Pinus nigra Arn. subsp. pallasiana under different climate conditions throughout western Anatolia, Dendrochronologia, 295-301, 2012.

Köse, N., Akkemik, U., Guner, H.T., Dalfes, H.N., Grissino-Mayer, H.D., Ozeren, M.S., Kindap, T.: An improved reconstruction of May– June precipitation using tree-ring data from western Turkey and its links to volcanic eruptions, Int. J. Biometeorol, 57(5), 691–701, 2013.

Lionello, P. (Ed.),:The Climate of the Mediterranean Region, from the Past to the Future. Elsevier, Amsterdam, Netherlands, 2012.

Luterbacher, J., Dietrich, D., Xoplaki, E., Grosjean, M., Wanner, H.:European seasonal and annual temperature variability, trends and extremes since 1500. Science, 303, 1499–1503, 2004.

Luterbacher, J., Werner, J.P., et al.: European summer temperatures since Roman times. Environmental Research Letters, 11: 024001, doi:10.1088/1748-9326/11/1/024001, 2016.

Martin-Benito, D., Ummenhofer C.C., Köse, N., Güner, H.T., Pederson, N.: Tree-ring reconstructed May-June precipitation in the Caucasus since 1752 CE, Clim. Dyn., DOI 10.1007/s00382-016-3010-1, 2016.

Meko, D. M. and Graybill, D. A.: Tree-ring reconstruction of upper Gila River discharge, Wat. Res. Bull., 31, 605–616, 1995.

Mutlu, H., Köse, N., Akkemik, Ü., Aral, D., Kaya, A., Manning, S. W., Pearson, C. L., and Dalfes, N.: Environmental and climatic signals from stable isotopes in Anatolian tree rings, Turkey, Reg. Emviron. Change, doi: 10.1007/s1011301102732, 2011.

Nicault, A., Alleaume, S., Brewer, S., Carrer, M., Nola, P., and Guiot, J.: Mediterranean drought fluctuation during the last 500 years based on tree-ring data, Clim. Dynam., 31(2–3), 227–245, 2008.

Orvis, K. H. and Grissino-Mayer, H. D.: Standardizing the reporting of abrasive papers used to surface tree-ring samples, Tree-Ring Res., 58, 47–50, 2002.

Pauling, A., Luterbacher, J., Casty, C., Wanner, H.: Five hundred years of gridded high-resolution precipitation reconstructions over Europe and the connection to large-scale circulation. Clim. Dynam., 26, 387–405, 2006.

Roberts, N., Moreno, A., Valero-Garces, B.L.: Palaeolimnological evidence for an east-west climate see-saw in the Mediterranean since AD 900. Glob. Planet. Change, 84, 23–34, 2012.

Sanchez-López, G. Hernandez, A., Pla-Rabes, et al.: Climate reconstruction for the last two millennia in central Iberia: The role of East Atlantic (EA), North Atlantic Oscillation (NAO) and their interplay over the Iberian Peninsula. Quaternary Science Reviews,149, 135–150, 2016.

Server, M.: Evaluation of an oral history text in the context of social memory and traditional activity, Milli Folklor 77, 61–68 (In Turkish), 2008.

Speer, J. H.: Fundamentals of Tree-Ring Research, University of Arizona Press, Tucson, 2010.

St. George, S.: An overview of tree-ring width records across the Northern Hemisphere, Quat. Sci. Rev., 95, 132–150, 2014.

St. George, S., and Ault. T. R.: The imprint of climate within northern hemisphere trees, Quat. Sci. Rev., 89, 1–4, 2014.

Stokes, M. A. and Smiley, T. L.: An Introduction to Tree-ring Dating, The University of Arizona Press, Tucson, 1996.

Till, C. and Guiot, J.: Reconstruction of precipitation in Morocco since A D 1100 based on *Cedrus atlantica* tree-ring widths, Quat. Res., 33, 337–351, 1990.

Touchan, R., Garfin, G. M., Meko, D. M., Funkhouser, G., Erkan, N., Hughes, M. K., and Wallin, B. S.: Preliminary reconstructions of spring precipitation in southwestern Turkey from tree-ring width, Int. J. Clim., 23, 157–171, 2003.

Touchan, R., Xoplaki, E., Funkhouser, G., Luterbacher, J., Hughes, M. K., Erkan, N., Akkemik, Ü., and Stephan, J.: Reconstruction of spring/summer precipitation for the Eastern Mediterranean from tree-ring widths and its connection to large-scale atmospheric circulation, Clim. Dynam., 25, 75–98, 2005a.

Touchan, R., Funkhouser, G., Hughes, M. K., and Erkan, N.: Standardized Precipitation Index reconstructed from Turkish ring widths, Clim. Change, 72, 339-353, 2005b.

Touchan, R., Akkemik, Ü., Huges, M. K., and Erkan, N.: May–June precipitation reconstruction of southwestern Anatolia, Turkey during the last 900 years from tree-rings, Quat. Res., 68, 196-202, 2007.

Turkes, M.: Spatial and temporal analysis of annual rainfall variations in Turkey, Int. J. Clim., 16, 1057–1076, 1996a.

Turkes, M.:. Meteorological drought in Turkey: a historical perspective, 1930–1993. In: Drought Network News, International Drought Information Center, University of Nebraska, 8, pp. 17–21, 1996b.

Turkes, M.: Vulnerability of Turkey to desertification with respect to precipitation and aridity conditions. Turk. J. Engineer. Environ Sci., 23, 363–380, 1999.

Turkes, M. and Sumer, U. M.: Spatial and temporal patterns of trends variability in diurnal temperature ranges of Turkey. Theor. Appl. Clim., 77, 195–227, 2004.

Xoplaki, E., Luterbacher J., Paeth H., Dietrich, D., Grosjean, M., Wanner, H.: European spring and autumn temperature variability and change of extremes over the last half millennium. Geophys. Res. Lett., 32, L15713, doi:10.1029/2005GL023424.

Wahl, E. R., Anderson, D. M., Bauer, B. A., Buckner, R., Gille, E. P., Gross, W. S., Hartman, M., and Shah, A.: An archive of high-resolution temperature reconstructions over the past two millennia, Geochem. Geophys. Geosyst., 11, Q01001, doi:10.1029/2009GC002817, 2010.

Wigley, T. M. L., Briffa, K. R., and Jones, P. D.: On the average value of correlated time series with applications in dendroclimatology and hydrometeorology, J. Clim. Appl. Met., 23, 201–213, 1984.

Yamaguchi, D. K.: A simple method for cross-dating increment cores from living trees. Can. J. For. Res., 21, 414–416, 1991.

Zücher, E. J.: Turkey: A modern history. Oxford Publishing Services, New York, 2004.

Table 1. Site information for the new chronologies developed by this study in Turkey.

Site name	Site code	Species	No. trees/ cores	Aspect	Elev. (m)	Lat. (N)	Long. (E)
Çorum, Kargı, Karakise kayalıkları	KAR	*Pinus nigra*	22 / 38	SW	1522	41°11'	34°28'
Çorum, Kargı, Şahinkayası mevkii	SAH	*P. nigra*	12 / 21	S	1300	41°13'	34°47'
Bilecik, Muratdere	ERC	*P. nigra*	12 / 25	SE	1240	39°53'	29°50'
Bolu, Yedigöller, Ayıkaya mevkii	BOL	*P. sylvestris*	10 / 20	SW	1702	40°53'	31°40'
Eskişehir, Mihalıççık, Savaş alanı mevkii	SAV	*P. nigra*	10 / 18	S	1558	39°57'	31°12'
Kayseri, Aladağlar milli parkı, Hacer ormanı	HCR	*P. nigra*	18 / 33	S	1884	37°49'	35°17'
Kahramanmaraş, Göksun, Payanburnu mevkii	PAY	*P. nigra*	10 / 17	S	1367	37°52'	36°21'
Artvin, Borçka, Balcı işletmesi	ART	*Abies nordmanniana* *Picea orientalis*	23 / 45	N	1200–2100	41°18'	41°54'

Table 2. Summary statistics for the new chronologies developed by this study in Turkey.

Total chronology				Common interval		
Site Code	Time span	1st year (*EPS > 0.85)	Mean sensitivity	Time span	Mean correlations: among radii /between radii and mean	Variance explained by PC1 (%)
KAR	1307–2003	1620	0.22	1740–1994	0.38 / 0.63	41
SAH	1663–2003	1738	0.25	1799–2000	0.42 / 0.67	45
ERC	1721–2008	1721	0.23	1837–2008	0.45 / 0.69	48
BOL	1752–2009	1801	0.18	1839–1994	0.32 / 0.60	36
SAV	1630–2005	1700	0.17	1775–2000	0.33 / 0.60	38
HCR	1532–2010	1704	0.18	1730–2010	0.38 / 0.63	40
PAY	1537–2010	1790	0.18	1880–2010	0.28 / 0.56	32
ART	1498–2007	1624	0.12	1739–1996	0.37 / 0.60	41

*EPS = Expressed Population Signal [Wigley et al., 1984]

Table 3. Principal components analysis statistics for the Turkey temperature reconstruction model.

	Explained variance (%)	Correlation coefficients with May–August PPT	Correlation coefficients with March–April TMP	The chronologies represented by higher magnitudes** in the eigenvectors
PC1	46.57	0.65	0.19	KAR, KIZ, TEF, BON,USA,TUR, CAT, INC, ERC, YAU, SAV, TAN, SIU
PC2	7.86	–0.07	0.15	KAR, SAV, TIR, BOL, YAU, ESK, TEF,BON, SIU
PC3*	4.93	0.04	–0.48	HCR, PAY, BOL, YAU, SIA
PC4*	4.68	0.11	0.17	TEF, KEL, FIR, SIA, KIZ, SIU, ART
PC5*	4.42	–0.25	0.27	SAH, TIR, FIR, ART
PC6	3.73	0.15	–0.14	KIZ, FIR, SAV, KAR, TIR, PAY, ESK, TEF, BON, ART
PC7*	3.56	0.19	0.18	KIZ, BON, BOL, YAU, HCR, PAY, INC
PC8	2.87	0.26	0.01	HCR, ESK, BON, FIR, ERC, SIA
PC9*	2.45	0.16	0.17	PAY, USA, BOL, YAU, TIR, HCR, FIR, SIA, SIU
PC10*	2.21	0.14	–0.08	TUR, CAT, SAV, SIA, KEL, ERC, SIU
PC11	2.09	–0.36	–0.20	HCR, TEF, USA, INC, PAY, TUR, SAV, SIU
PC12	1.80	–0.12	0.05	TEF, CAT, YAU HCR, ESK, USA, BOL, SIA
PC13	1.63	–0.06	0.17	TEF, TUR, BOL, KAR, YAU, SIA
PC14	1.55	–0.14	0.06	TIR, USA, FIR, TUR, YAU, KAR, BON
PC15*	1.50	–0.20	–0.14	KIZ, BON, USA, ESK, INC, BOL
PC16	1.31	0.04	0.08	SAH, HCR, INC, YAU, SAV, KAR, FIR, BOL, SIU
PC17*	1.25	0.15	0.19	SAH, SIU, KAR, ESK, TUR, ERC
PC18	1.14	0.13	0.02	KAR, TEF, TUR, SAV, BON, CAT
PC19	1.09	0.16	–0.11	PAY, INC, SAV, HCR, KEL, CAT, TAN
PC20	0.95	–0.15	–0.01	TIR, SAH, CAT
PC21*	0.89	0.06	–0.28	TUR, INC, TIR, SAV
PC22	0.85	0.44	0.10	KIZ, SAH, BON, YAU, SIU
PC23	0.67	–0.22	–0.02	TAN, KEL, TUR, CAT

"*" indicates the PCs, which used in the reconstruction as predictors

"**" which exceed ±0.2 value.

Table 4. Calibration and verification statistics of bootstrap method (1000 iterations applied) showing the mean values based on the 95% confidence interval (CI).

		Mean (95% CI)
Calibration	RMSE	0.65 (0.52; 0.77)
	R^2	0.73 (0.60; 0.83)
Verification	RE	0.54 (0.15; 0.74)
	CE	0.51 (0.04; 0.72)
	RMSEP	0.88 (0.67; 1.09)

RMSE root mean squared error; R^2 coefficient of determination; *RE* reduction of error; *CE* coefficient of efficiency; *RMSEP* root mean squared error prediction

Table 5. Calibration and cross-validation statistics for the Turkey temperature reconstruction model.

Calibration Period	Verification Period	Adj. R^2	F	RE	CE
1930–1966	1967–2002	0.55	5.91 $p \leq$ 0.0001	0.64	0.58
1967–2002	1930–1966	0.71	10.45 $p \leq$ 0.0001	0.63	0.46

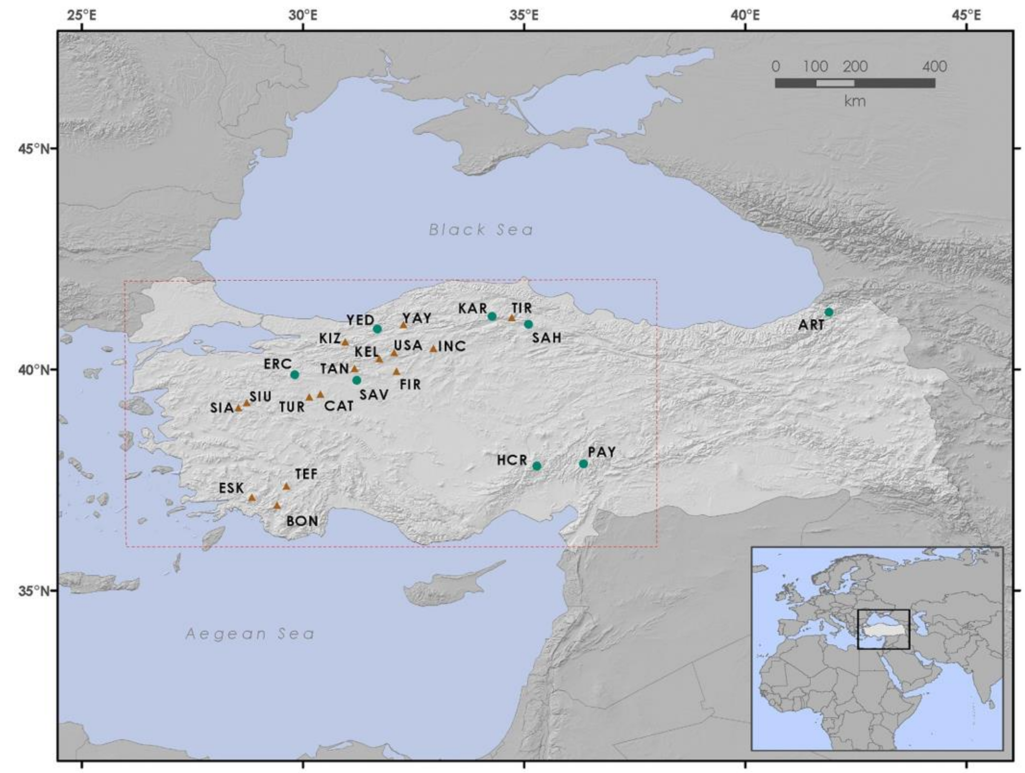

Figure 1. Tree-ring chronology sites in Turkey used to reconstruct temperature. Circles represent the new sampling efforts from this study and the triangles represent previously-published chronologies (YAY, SIA, SIU: Mutlu et al. 2011; TIR: Akkemik et al. 2008; TAN: Köse et al. unpublished data; KIZ, ESK, TEF, BON, KEL, USA, FIR, TUR: Köse et al. 2011; CAT, INC: Köse et al. 2005). The box (dashed line) represents the area for which the temperature reconstruction was performed.

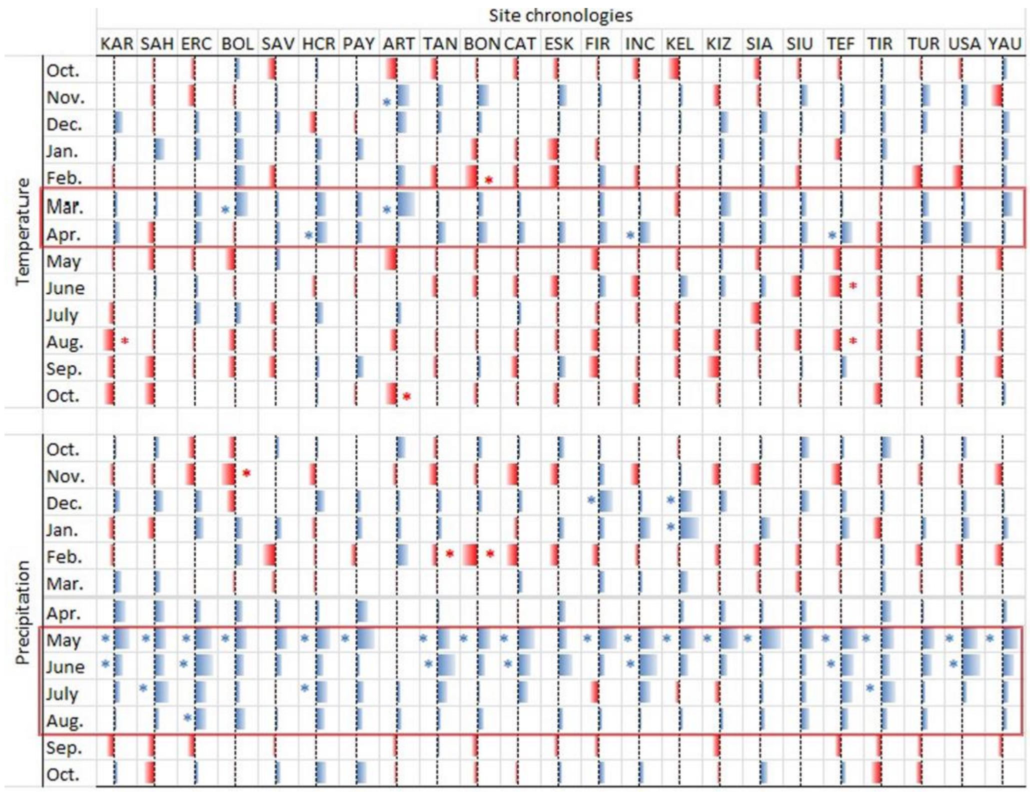

Figure 2. Summary of response function results of 23 chronologies. Red color represents negative effects of climate variability on tree ring width; blue color represents positive effects of climate variability on tree ring width. "*" indicates statistically significant response function confidents (p ≤≤ 0.05). Each response function includes 13 weights for average monthly temperatures and 13 monthly precipitations from October of the prior year to October of current year.

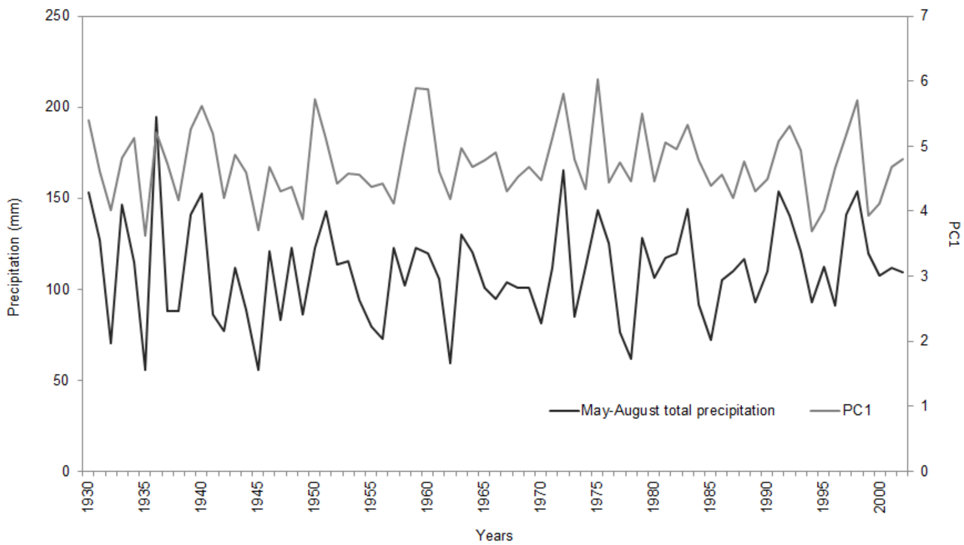

Figure 3. The comparison of May–August total precipitation (black) and the first principal component of 23 tree-ring chronologies (gray). Correlation coefficient between two time series is 0.65 (*p* < 0.001).

Biçimlendirilmiş: Yazı tipi: İtalik

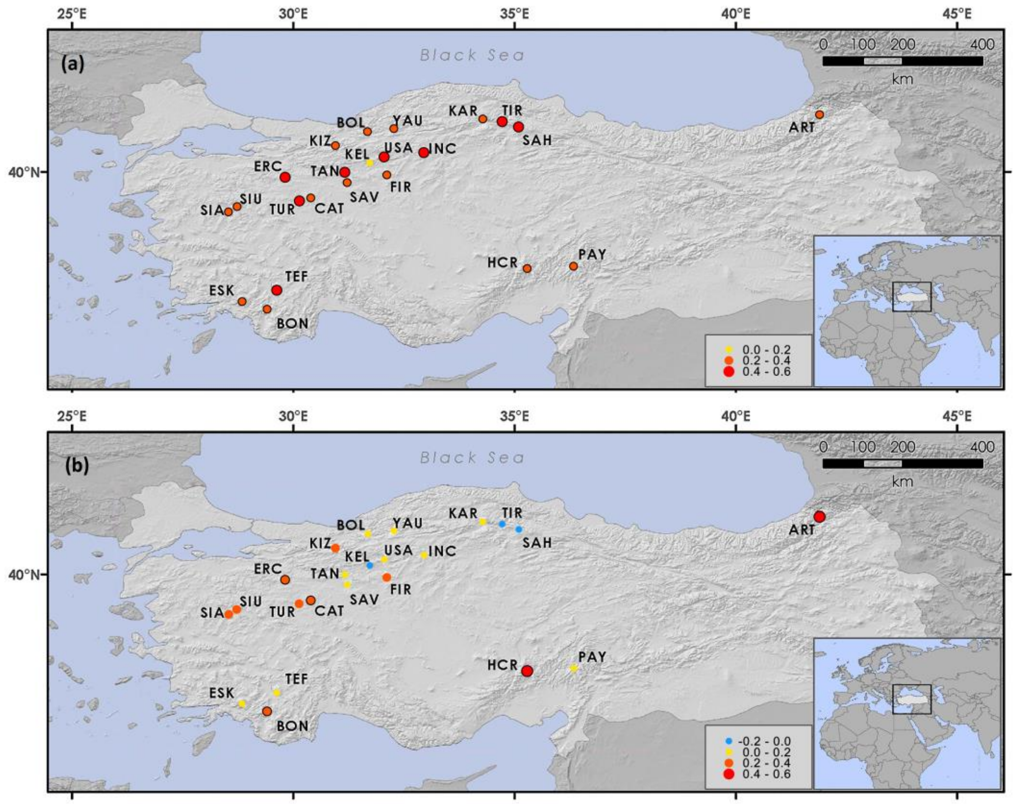

Figure ~~3~~4. Maps showing Pearson's correlation coefficients between the sites chronologies and (a) May–August total precipitation and (b) March-April mean temperature for the period 1930–2012. For each site, the closest gridded (0.5° x 0.5°) climate data obtained from CRU dataset were used. Graduated circle size and color correspond to correlation coefficient versus the climate variable. Black lines surrounding circles represent significant correlation coefficients ($p < 0.05$).

Biçimlendirilmiş: Yazı tipi: İtalik

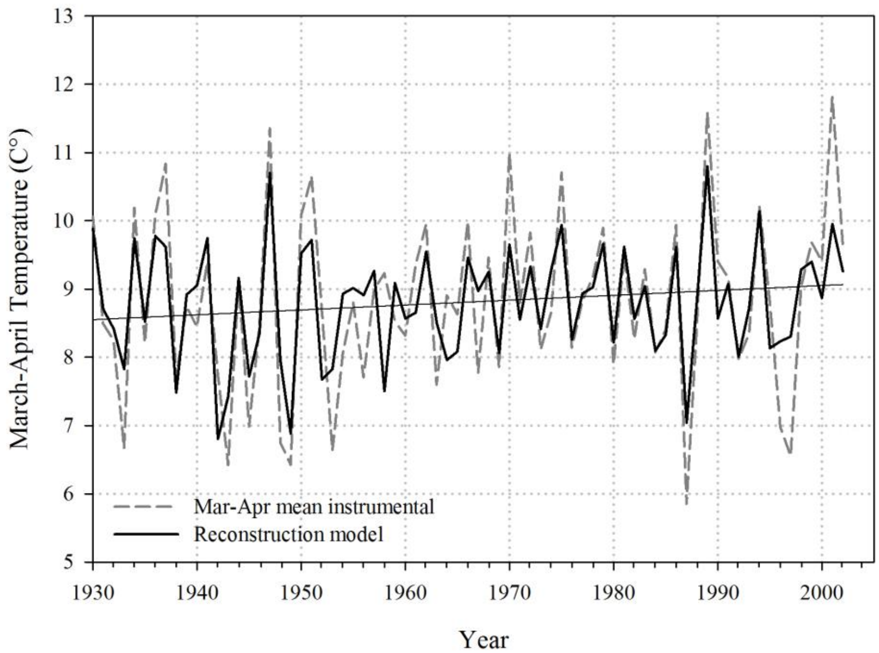

Figure 5. Actual (instrumental) and reconstructed March–April temperature (°C). Dashed lines (dark grey) represent actual values and solid lines (black) represent reconstructed values shown with trend line (linear black line). Note: y-axes labels range 5–13 °C.

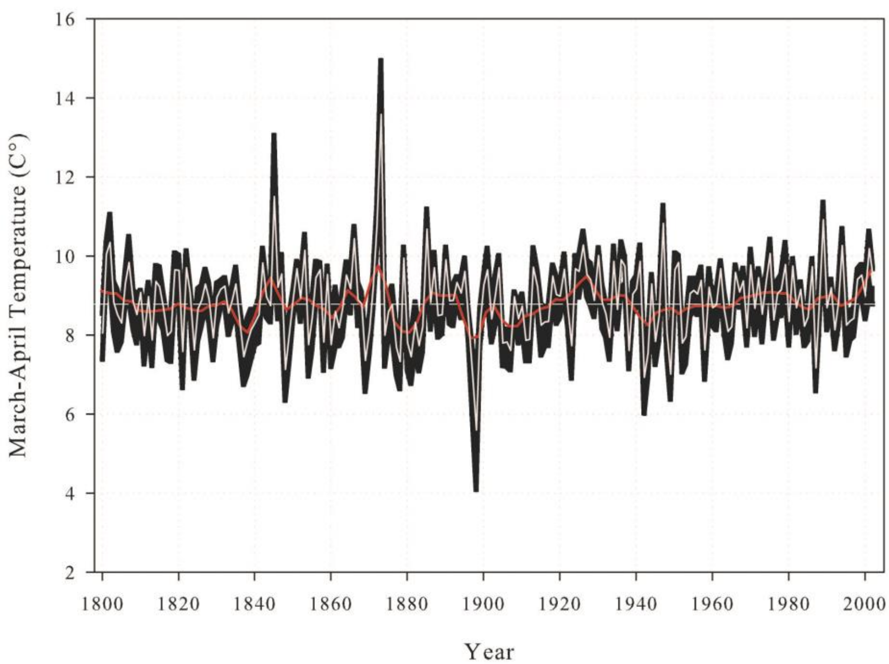

Figure 6. March–April temperature reconstruction for Turkey for the period 1800–2002 CE. The central horizontal line (dashed white) shows the reconstructed long-term mean; ~~dark grey~~black background denotes Monte Carlo (*n* = 1000) bootstrapped 95% confidence limits; and the ~~solid black~~red line shows 13-year low-pass filter values. Note: y-axis labels range 2–16 °C.

Biçimlendirilmiş: Yazı tipi: Times New Roman

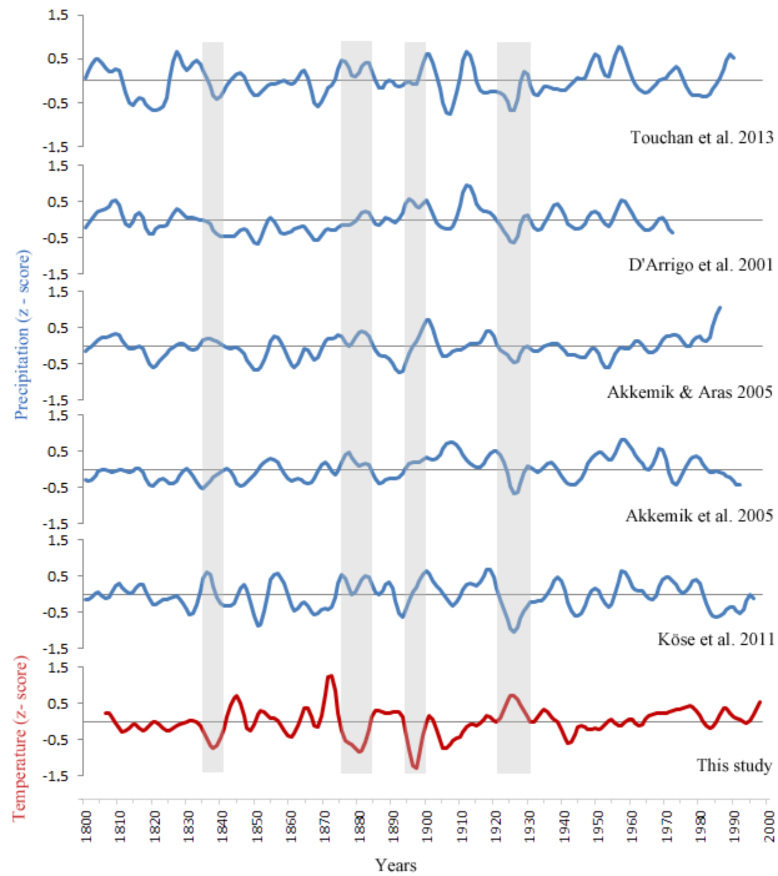

Figure 7. Low-frequency variability of previous tree-ring based precipitation reconstructions from Turkey and spring temperature reconstruction. Each line shows 13-year low-pass filter values. z-scores were used for comparison.

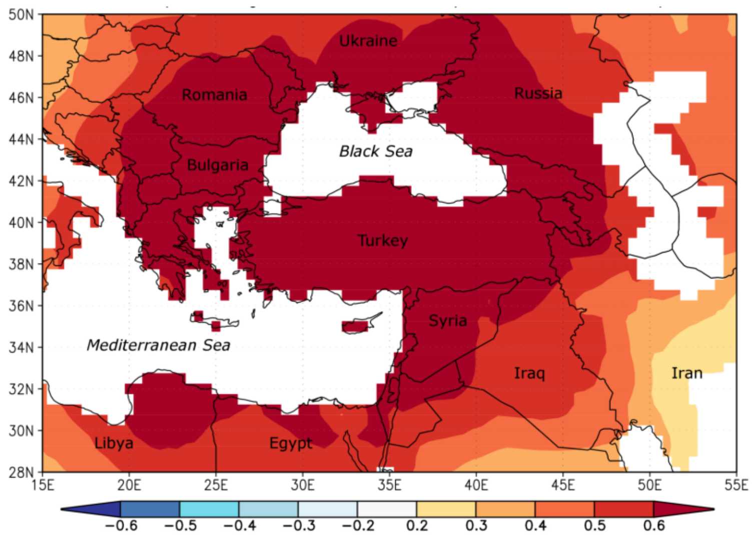

Figure 8. Spatial correlation map for the March–April temperature reconstruction. Spatial field correlation map showing statistical relationship between the temperature reconstruction and the gridded temperature field at 0.5º intervals (CRU TS3.23; Jones and Harris 2008) during the period 1930–2002 over the Mediterranean region. For each grid, calculated correlation coefficient from 0.20 to 0.60 is significant ($p < 0.05$).

Biçimlendirilmiş: Yazı tipi: İtalik

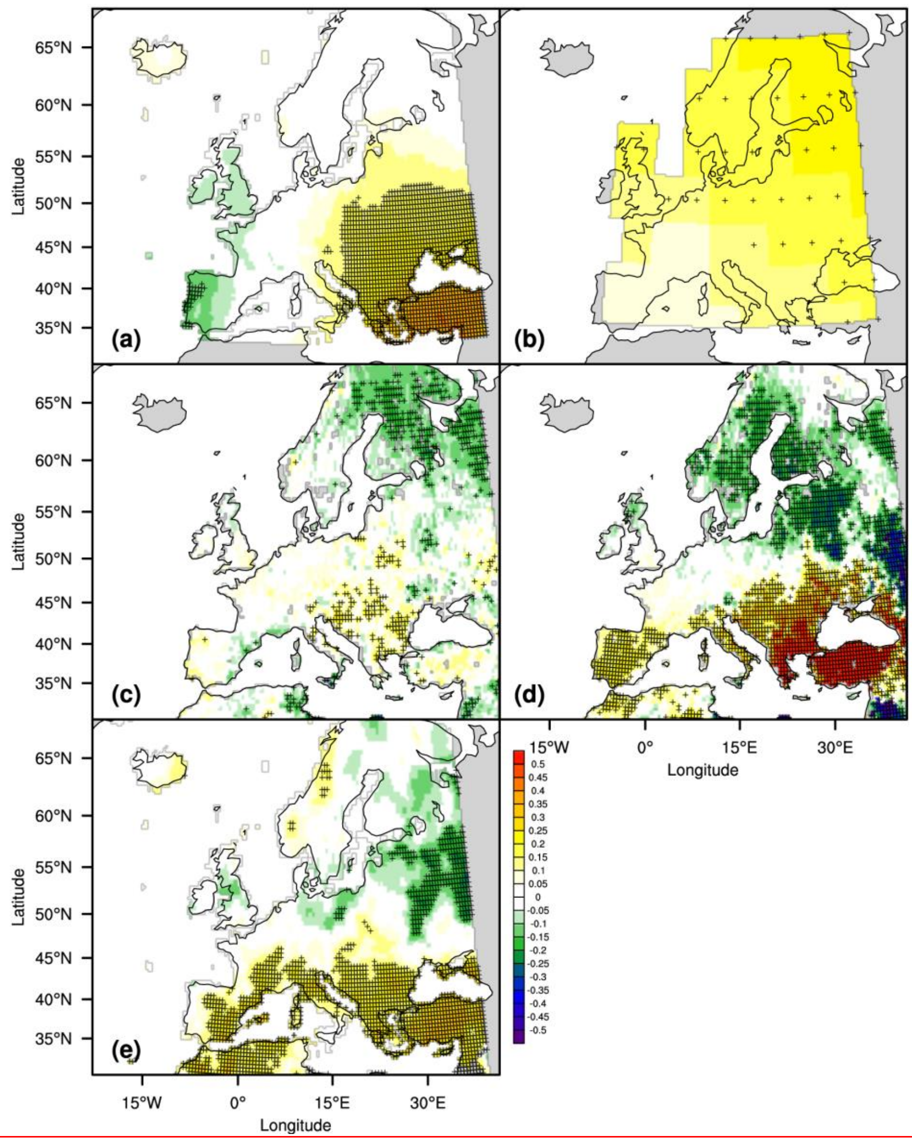

Figure 9. Spatial correlation maps for the March–April temperature reconstruction and precipitation signal (PC1) obtained from tree-ring data set during the period 1800–2002 over Europe. Maps demonstrate spatial field correlations between our temperature

reconstruction and (a) gridded spring temperature reconstruction for Europe (Xoplaki et al. 2005), (b) gridded summer temperature reconstruction for Europe (Luterbacher et al. 2016), (c) Old World Drought Atlas (OWDA; Cook et al. 2015). Panels (d) and (e) show spatial correlations between PC1 and OWDA (Cook et al. 2015) and gridded European summer precipitation reconstruction (Pauling et al., 2006), respectively. '+' represents significant correlation coefficients ($p < 0.05$).

Biçimlendirilmiş: Yazı tipi: İtalik

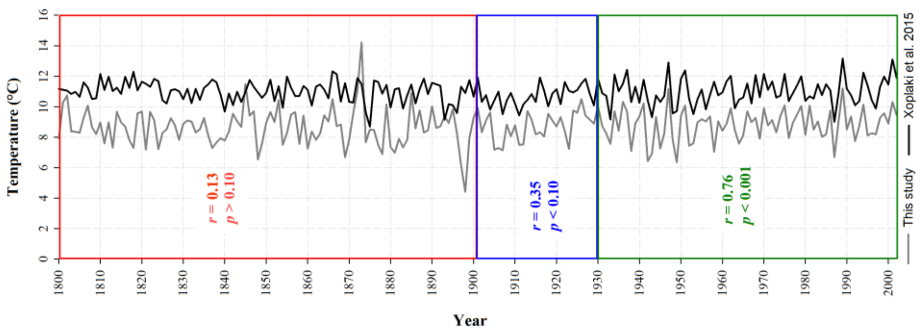

Figure 10. Comparison of March-April temperature reconstruction (gray) with the mean of corresponding grid points from European spring (March to May) temperature reconstruction (Xoplaki et al. 2005; black) over the study area (36–42º N, 26–38º E). The indicated correlation coefficients are calculated for instrumental period (also calibration period for this study) (1930–2002; $r = 0.76$, $p < 0.001$); for the pre-instrumental period of Turkey, while instrumental data has sufficient quality for most part of Europe (1901–1929; $r = 0.35$, $p < 0.10$); and for pre-instrumental period (1800–1900; $r = 0.13$, $p < 0.10$).

Biçimlendirilmiş: Yazı tipi: İtalik

Biçimlendirilmiş: Yazı tipi: İtalik

Biçimlendirilmiş: Yazı tipi: İtalik

Biçimlendirilmiş: Yazı tipi: İtalik

Biçimlendirilmiş: Yazı tipi: İtalik

Biçimlendirilmiş: Yazı tipi: İtalik